한국정밀공학회지 제 38 권 제 2 호 pp. 115-122 February 2021 / 115
J. Korean Soc. Precis. Eng., Vol. 38, No. 2, pp. 115-122 http://doi.org/10.7736/JKSPE.020.077
ISSN 1225-9071 (Print) / 2287-8769 (Online)

Super-Twisting 제어기법 기반 짐벌운동제어시스템 설계에 관한 연구

A Study on Gimbal Motion Control System Design based on Super-Twisting Control Method

틴 휭[1], 김영복[2,#]
Thinh Huynh[1] and Young-Bok Kim[2,#]

1 부경대학교 대학원 스마트로봇융합응용공학과 (Department of Smart Robot Convergence & Application Engineering, Graduate School, Pukyong National University)
2 부경대학교 기계시스템공학과 (Department of Mechanical System Engineering, Pukyong National University)
Corresponding Author / E-mail: kpjiwoo@pknu.ac.kr, TEL: +82-51-629-6197
ORCID: 0000-0001- 6035-6744

KEYWORDS: Gimbal (짐벌), Line of sight (LOS), Inertial stabilization (관성안정화), Super-twisting algorithm (슈퍼-트위스팅 알고리즘), Sliding mode control (슬라이딩모드제어)

Controlling an optical sensor's line of sight (LOS) with an inertial stabilization system carried out on a dynamic platform is a challenging engineering task. The LOS needs to track a target object accurately despite intentional maneuvers, inadvertent motions, and additional disturbances. In this study, a super-twisting sliding mode controller (STSMC) is implemented to overcome this problem. The controller is designed based on the analysis of system dynamics. The stability is then proved to be satisfactory by the Lyapunov theory. Then, the control law is validated through experimental studies. In addition, a comparison to the performance of a linear controller is derived so that the effectiveness of the proposed controller is validated.

Manuscript received: August 8, 2020 / Revised: November 10, 2020 / Accepted: November 14, 2020

NOMENCLATURE

ω = Angular Velocity
φ = Angular Position
T = Torque
K = Viscous Friction Coefficient
Q = Cable Restrain Coefficient
J = Inertia Moment
u = Control Signal
s_i = Sliding Manifold
V = Lyapunov Function

1. Introduction

The main goal of an inertial stabilization is to hold or control the LOS of one object relative to another object or inertial space (Hilkert[1]). It is used in a large range of applications, such as surveillance, target tracking, communications, handheld cameras, etc. The optical sensor is carried by a gimbaled structure with at least two orthogonal axes. In direct stabilization system, the sensor is considered as the payload mounted in the inner gimbal channel where its absolute motion is sensed by a gyroscope and the gimbal motions are actuated by two independent servo systems. When disturbances affect the LOS are attenuated, the system can achieve accurate tracking performance with a well-designed controller. In the case of the gimbal carried on a mobile vehicle, disturbances arise from both intentional maneuvers and inadvertent motions of the vehicle. In addition, external loads, such as wind, friction, and mass unbalance, add unpredicted perturbations into the system.

Modern control techniques based on sliding mode control are well known as robust and effective methods to be applied in these

situations. However, chattering is the main drawback of the technique. In applications of inertial stabilization, many approaches based on sliding mode control have been proposed. For example, in the works of Kürkçü[2] and Li,[3] the use of an integral sliding mode controller combined with a disturbance/uncertainty estimator[2] or a state observer[3] were suggested. In Mao[4] and Suoliang,[5] controllers were designed based on terminal sliding mode algorithm. A combination of back-stepping control and sliding mode control was proposed in Dong[6] and Ding.[7]

Besides that, super-twisting algorithm not only provides finite-time convergence but also reduces chattering effects (Chalanga[8]). Tran[9] showed that super-twisting algorithm could be applied for inter-connected systems and performed well. Chanlanga[8] studied an output feedback stabilization of perturbed double-integrator systems using super-twisting control. Two methodologies were proposed, one was super-twisting controller based on super-twisting observer, and the other was high-order sliding mode observer based super-twisting controller. While the first approach was proved mathematically that it was impossible to achieve second order sliding on the control sliding variable, the second approach could achieve continuous control with super-twisting algorithm. Applying these results, Reis, et al., designed a sliding mode control strategy for both stabilization and target tracking for 3-DOF inertial stabilization (Reis[10]). Both state and output feedback cases were considered. The full state feedback values were represented in form of quaternions, while a high-order sliding mode observer was proposed to estimate velocities from the outputs. In each case, two super-twisting controllers were employed in cascade topology, providing robust and effective performance evaluated by simulation results. On the other hand, the main difficulty with super-twisting technique is to establish the proof of stability for perturbed systems. Studies of Levant,[11] Moreno[12,13] and other authors have suggested several rules for tuning controller gains such that system becomes stable. Especially, a recent study from Seeber[14] provided a strict Lyapunov function which extends the provably stable parameter range, even for the system with unmatched disturbances.

However, above-mentioned studies related to super-twisting sliding mode control are either theoretical or simulation ones. In order to tackle effectively the problem of tracking in two-axis gimbal system, a practical approach for design and implement of the super-twisting sliding mode controller is needed. In this work, the problem is solved and presented as follows. Section 2 derives system's mathematical model from the analysis of its kinematics and dynamics. Section 3 presents the procedure of super-twisting controller design from the system's model. Section 4 provides stability proof encouraged from the work of Seeber and Horn. The system with proper choice of parameters is proved to be finite-time stable in the sense of Lyapunov stability theory despite of the present of disturbances. Section 5 suggests some modifications improving the robustness and effectiveness of the implemented controller. Experimental studies validating the proposed controller are discussed in Section 6. Experimental results are analyzed and compared in this section. Finally, conclusions will be drawn.

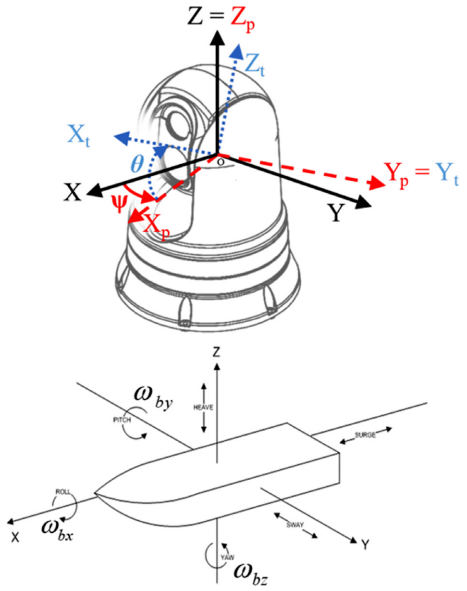

Fig. 1 A two-axis gimbal mounted on a vessel

2. System Modeling

Consider a two-axis gimbal mounted on a dynamics platform illustrated in Fig. 1. The gimbal consists of an outer channel actuating pan motion and an inner channel operating tilt motion. The first step of controller design process for this system is to build up the mathematical model which characterizes the kinematics and dynamics of it. By using the Euler matrix for rotations, the angular rates of the pan and tilt channels can be respectively written as Eq. (1).

$$\begin{bmatrix}\omega_{px}\\ \omega_{py}\\ \omega_{pz}\end{bmatrix}=\begin{bmatrix}C\psi & S\psi & 0\\ -S\psi & C\psi & 0\\ 0 & 0 & 1\end{bmatrix}\begin{bmatrix}\omega_{bx}\\ \omega_{by}\\ \omega_{bz}\end{bmatrix}+\begin{bmatrix}0\\ 0\\ \dot{\psi}\end{bmatrix}=\begin{bmatrix}\omega_{bx}C\psi+\omega_{by}S\psi\\ -\omega_{bx}S\psi+\omega_{by}C\psi\\ \omega_{bz}+\dot{\psi}\end{bmatrix} \quad (1)$$

$$\begin{bmatrix}\omega_{tx}\\ \omega_{ty}\\ \omega_{tz}\end{bmatrix}=\begin{bmatrix}C\theta & 0 & -S\theta\\ 0 & 1 & 0\\ S\theta & 0 & C\theta\end{bmatrix}\begin{bmatrix}\omega_{ox}\\ \omega_{oy}\\ \omega_{oz}\end{bmatrix}+\begin{bmatrix}0\\ \dot{\theta}\\ 0\end{bmatrix}=\begin{bmatrix}C\theta\left(\omega_{bx}C\psi+\omega_{by}S\psi\right)-S\theta(\omega_{bz}+\dot{\psi})\\ -\omega_{bx}S\psi+\omega_{by}C\psi+\dot{\theta}\\ S\theta\left(\omega_{bx}C\psi+\omega_{by}S\psi\right)+C\theta(\omega_{bz}+\dot{\psi})\end{bmatrix}$$

Where S and C denote for sine and cosine respectively,

$\omega_b = [\omega_{bx} \ \ \omega_{by} \ \ \omega_{bz}]^T$ is the angular rate of the platform, $\dot{\psi}$ is the relative rate between the outer gimbal and the platform along Z-axis, and $\dot{\theta}$ is the relative rate between the inner and outer gimbal along Y-axis. Next, the gimbal dynamics can be derived from the torque relationships about the inner and outer gimbal body axes. Euler's equation for rigid body dynamics is given by Eq. (2).

$$J\dot{\omega} + \omega \times (J\omega) = T \tag{2}$$

Where T is the applied torque, J is the matrix of inertia, and ω is the angular velocity.

To simplify the analysis, assume that the inner gimbal rotation axes are aligned with the principal axes of inertia so that its inertia matrix is diagonal $J_t = diag\{J_{tx},\ J_{ty},\ J_{tz}\}$ and assume $J_{tx} = J_{tz}$. Applying Eqs. (1) and (2), the inner gimbal dynamics about Y-axis and the outer gimbal dynamics about Z-axis are expressed as Eqs. (3) and (4).

$$J_{ty}\ddot{\varphi}_{ty} + K_{ty}\dot{\varphi}_{ty} + Q_{ty}\varphi_{ty} = T_{ty} - T_{dty} \tag{3}$$

$$(J_{pz} + J_{tx})\ddot{\varphi}_{pz} + K_{pz}\dot{\varphi}_{pz} + Q_{pz}C\theta\int_0^t \frac{1}{C\theta}\dot{\varphi}_{pz}d\tau = T_{pz}C\theta - T_{dpz} \tag{4}$$

Where ty and pz are index terms denoting elements corresponding to tilt motion about Y-axis and pan motion about Z-axis respectively. φ stands for angular position of LOS, J is inertia matrix element, K and Q are viscous friction coefficient and cable restrain coefficient respectively. T is control torque and T_d indicates additional disturbance torques. Disturbances in each channel consist of mass unbalance torque T_U, non-linear parts of friction T_K and cable restrain T_Q torques, platform maneuver torques transmitted to the channel T_b, and mutual interference between two channels (Kennedy,[15] Ekstrand[16] and Mokbel[17]).

$$\begin{aligned} T_{dty} &= T_{Ut} + T_{Kt} + T_{Qt} + T_{bt} + T_{pt} \\ T_{dpz} &= C\theta\left(T_{Up} + T_{Kp} + T_{Qp}\right) + T_{bp} + T_{tp} \end{aligned} \tag{5}$$

For the sake of simplification, let us consider the case that the relative angle between the inner and outer gimbal does not change when the outer gimbal is moving. Hence, Eq. (4) becomes Eq. (6).

$$(J_{pz} + J_{tx})\ddot{\varphi}_{pz} + \left(K_{pz} + P_{pz}\right)\dot{\varphi}_{pz} + Q_{pz}\varphi_{pz} = T_{pz}C\theta - T_{dpz} \tag{6}$$

3. Control System Design

3.1 Tracking Control System

Typical control configurations for inertial stabilization use two control loops: inner stabilization loop and outer tracking loop (Masten[18]). With the use of a simple P controller for stabilization, the control torques applied to actuators are generated as Eq. (7).

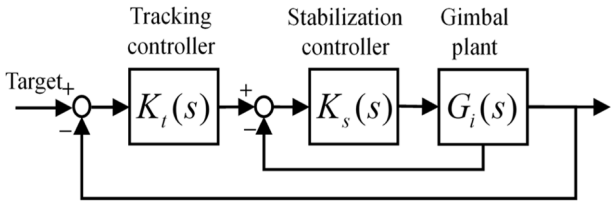

Fig. 2 Typical control configurations for inertial stabilization

$$\begin{aligned} T_{ty} &= P_{ty}\left(\dot{\theta}_d - \dot{\theta}\right) \\ T_{pz} &= P_{pz}\left(\dot{\psi}_d - \dot{\psi}\right) \end{aligned} \tag{7}$$

Where P are the gains of inner loop controller, $\dot{\theta}_d$ and $\dot{\psi}_d$ are desired relative angular rate. Thus, $\dot{\theta}_d$ and $\dot{\psi}_d$ are the references of inner control loop, which are also the control signals from outer tracking controller. Substituting Eq. (7) into Eqs. (3) and (6), and consider Eqs. (1) and (2) yields that:

$$\begin{aligned} &J_{ty}\ddot{\varphi}_{ty} + \left(K_{ty} + P_{ty}\right)\dot{\varphi}_{ty} + Q_{ty}\varphi_{ty} = P_{ty}\dot{\theta}_d - T_{dty} - P_{ty}\left(-\omega_{bx}S\psi + \omega_{by}C\psi\right) \\ &(J_{pz} + J_{tx})\ddot{\varphi}_{pz} + \left(K_{pz} + P_{pz}\right)\dot{\varphi}_{pz} + Q_{pz}\varphi_{pz} = P_{pz}C\theta\dot{\psi}_d - T_{dpz} \\ &\qquad - P_{pz}C\theta\left[\frac{\left(\omega_{bx}C\psi + \omega_{by}S\psi\right)S\theta}{C\theta} + \omega_{bxz}\right] \end{aligned} \tag{8}$$

Therefore, the procedure of tracking controllers design considers Eq. (8) as the plant, which contains a closed-loop system consisted of the gimbal plant and stabilization controller.

3.2 Super-Twisting Sliding Mode Controller Design

The idea behind sliding mode control algorithm is to design a feedback control law such that control error remains on well behaved sliding manifold despite the presence of the model imprecision and of disturbances. In order to design the tracking controller for the gimbal, let us consider the general description of each channel rewritten as follow Eq. (9).

$$\ddot{\varphi}_i + a_i\dot{\varphi}_i + b_i\varphi_i = c_i u_i - T_{di} \tag{9}$$

Where i = 1, 2 are the index of tilt channel and pan channel respectively; a, b, and c are nominal parameters of the system model corresponding to system dynamics, u is the control signal of proposed tracking controller and T_d is the total disturbance.

Firstly, a sliding manifold for each channel is assigned as follows Eq. (10).

$$s_i = \dot{e}_i + m_i e_i \tag{10}$$

Where $e_i = \varphi_{di} - \varphi_i$ is the tracking error - the difference between desired position φ_{di} and actual position φ_i. With $m_i > 0$, s_i is Hurwitz.

Take the time derivative of s_i and substitute from Eq. (9).

$$\begin{aligned}\dot{s}_i &= \ddot{e}_i + m_i \dot{e}_i \\ &= \ddot{\varphi}_{di} - \ddot{\varphi} + m_i \dot{e}_i \\ &= \ddot{\varphi}_{di} - c_i u_i + a_i \dot{\varphi}_i + b_i \varphi_i + m_i \dot{e}_i + T_{di}\end{aligned} \tag{11}$$

Then, a feedback control law is selected based on Super-Twisting algorithm in order to satisfy sliding condition, $\dot{s}_i = 0$, taking present of disturbance into account, as follows Eq. (12).

$$u_i = \frac{1}{c_i}\left(u_{iSM} + u_{iST}\right) \tag{12}$$

where

$$\begin{aligned}u_{iSM} &= \ddot{\varphi}_{di} + a_i \dot{\varphi}_i + b_i \varphi_i + m_i \dot{e}_i \\ u_{iST} &= \lambda_{1i} |s_i|^{1/2} \operatorname{sign}(s_i) + z_i \\ \dot{z}_i &= \lambda_{2i} \operatorname{sign}(s_i)\end{aligned} \tag{13}$$

with λ_{1i} and λ_{2i} are positive constants so that the system is stable and well performance.

Substituting the control law into equation of sliding manifold surface yields that Eq. (14).

$$\begin{aligned}\dot{s}_i &= -\lambda_{1i} |s|^{1/2} \operatorname{sign}(s_i) + x_i + T_{ui} \\ \dot{x}_i &= -\lambda_{2i} \operatorname{sign}(s_i) + \dot{T}_{mi}\end{aligned} \tag{14}$$

$T_{di} = T_{mi} + T_{ui}$ denotes that in general, unknown disturbances consist of matched disturbances T_{mi} and unmatched disturbances T_{ui}.

4. System Stability Analysis

Assume that the unmatched disturbances can be expressed as $\eta|s_i|^{1/2}$, and disturbances are bounded by non-negative constants $|\eta| \le N$ and $|\dot{T}_{mi}| \le L$. Consider the Lyapunov candidate as Eq. (15).

$$V = \begin{cases} 2\sqrt{x_i^2 + 3\alpha_i^2 \lambda_{1i}^2 |s_i|} - x_i \operatorname{sign}(s_i) & x_i \operatorname{sign}(s_i) \le \alpha_i \lambda_{1i} \sqrt{|s_i|} \\ 3|x_i| & \text{otherwise} \end{cases} \tag{15}$$

where α_i is a positive parameter. This function is continuous, positive definite, piecewise differentiable and locally Lipschitz continuous everywhere except in the origin (Seeber[14]).

In detail, in the first case, in the subdomain of semi-positive values of s_i, the function $2\sqrt{x_i^2 + 3\alpha_i^2 \lambda_i^2 s_i} - x_i$ is used, and in the subdomain of negative values of s_i, the function $2\sqrt{x_i^2 - 3\alpha_i^2 \lambda_i^2 s_i} + x_i$ is used. Both are continuously differentiable. The similar conclusion is obtained for the other case. Therefore, V is piecewise differentiable.

In the first case, $x_i \operatorname{sign}(s_i) \le \alpha_i \lambda_{1i} \sqrt{|s_i|}$, consider $s_i \ge 0$, and take time derivative of V.

$$\dot{V} = (\lambda_{2i} - \dot{T}_{mi}) + \frac{3\alpha_i^2 \lambda_{1i}^2 \left(x_i - \lambda_{1i}\sqrt{s_i} + \eta\sqrt{s_i}\right) - 2x_i\left(\lambda_{2i} - \dot{T}_{mi}\right)}{\sqrt{x_i^2 + 3\alpha_i^2 \lambda_{1i}^2 s_i}} \tag{16}$$

$\dot{V}$ is a homogeneous function of degree zero with respect to $\sqrt{s_i}$ and x_i. Then, the function's behavior for values of x_i satisfying $x_i^2 + 3\alpha_i^2 \lambda_{1i}^2 s_i = 1$ should be hold for any greater range of x_i. One consequently, defines the function.

$$\begin{aligned}g(x_i) &:= \dot{V}\big|_{x_i^2 + 3\alpha_i^2 \lambda_{1i}^2 s_i = 1} \\ &= (\lambda_{2i} - \dot{T}_{mi})(1 - 2x_i) + 3\alpha_i^2 \lambda_{1i}^2 x_i \\ &\quad - \alpha_i \lambda_{1i}^2 \sqrt{3 - 3x_i^2} + \alpha_i \lambda_{1i} \eta \sqrt{3 - 3x_i^2}\end{aligned} \tag{17}$$

The restrictions $s_i \ge 0$ and $x_i \le \alpha_i \lambda_{1i} \sqrt{s_i}$ are equivalent to the argument x_i of this function lying in the interval [-1, 1/2]. The second derivative of Eq. (17) is:

$$\frac{d^2 g}{dx_i^2} = \frac{\alpha_i \lambda_{1i}}{\left(1 - x_i^2\right)\sqrt{3 - 3x_i^2}}\left(1 + 2x_i^2\right)\left(\lambda_{1i} - \eta\right) \tag{18}$$

It can be seen that with $\lambda_{1i} \ge N$, $d^2g/dx_i^2 \ge 0$, then $g(x_i)$ is convex. Therefore:

$$g(x_i) \le \max\left(g(-1), g\left(\frac{1}{2}\right)\right) \tag{19}$$

where

$$\begin{aligned}g(-1) &= 3(\lambda_{2i} - \dot{T}_{mi} - \alpha_i^2 \lambda_{1i}^2) \le 3(\lambda_{2i} + L - \alpha_i^2 \lambda_{1i}^2) \\ g(\tfrac{1}{2}) &= \frac{3}{2}\alpha_i \lambda_{1i}\left(\alpha_i \lambda_{1i} - \lambda_{1i} + \eta\right)\end{aligned} \tag{20}$$

Thus, by homogeneity one concludes that:

$$\dot{V} \le \max\left(3(\lambda_{2i} + L - \alpha_i^2 \lambda_{1i}^2), \frac{3}{2}\alpha_i \lambda_{1i}\left(\alpha_i \lambda_{1i} - \lambda_{1i} + \eta\right)\right) \tag{21}$$

The system stability is preserved if $\dot{V} < 0$, then controller gains must satisfy

$$0 < \alpha_i < 1 - \frac{\eta}{\lambda_{1i}} \tag{22}$$

and

$$\lambda_{1i} > N + \sqrt{\lambda_{2i} + L} \tag{23}$$

If $s_i < 0$, the same conclusion is obtained by a similar procedure.

Furthermore, in the case of $x_i \text{sign}(s_i) > \alpha_i \lambda_{1i} \sqrt{|s_i|}$, time derivative of V yields that:

$$\begin{aligned} \dot{V} &= 3sign(x_i)\left(-\lambda_{2i} sign(s_i) + \dot{T}_{dim}\right) \\ &= 3sign(x_i s_i)\left(-\lambda_{2i} + \frac{\dot{T}_{dim}}{sign(s_i)}\right) < 3\left(L - \lambda_{2i}\right) \end{aligned} \tag{24}$$

$$\dot{V} < 0 \text{ if and only if } \lambda_{2i} > L \tag{25}$$

From Eqs. (23) and (25), the system is finite time stable if the conditions $\lambda_{2i} > L$ and $\lambda_{1i} > N + \sqrt{\lambda_{2i} + L}$ are satisfied.

As a result, with the proper choice of gain values, the stability of closed - loop system is preserved in the sense of Lyapunov stability theory despite of the present of disturbances.

5. Implementation

Chattering is well known as one of the main disadvantages of sliding mode controller. It has been shown that this effect is mainly caused by unmodelled cascade dynamics which increase the system's relative degree and perturb the ideal sliding mode existing in the system (Fridman[19]).

By including an integrator, the Super-Twisting algorithm is able to attenuate chattering in relative degree one system. In order to reduce the influence of higher relative degree, the proposed control law is calculated from a continuous signum-like function instead of the sign function.

$$\begin{aligned} u_{iST} &= \lambda_{1i} |s_i|^{1/2} \text{sgn}(s_i, \delta_i) + z_i \\ \dot{z}_i &= \lambda_{2i} \text{sgn}(s_i, \delta_i) \end{aligned} \tag{26}$$

Where $\text{sgn}(s_i, \delta_i)$ is defined as $\text{sgn}(s_i, \delta_i) = \frac{s_i}{|s_i| + \delta_i}$, δ_i is a positive constant.

6. Experiment

Experimental studies are performed on a two-axis gimbal used in ocean surveillance applications. Nominal parameters of the system defined in Eq. (9) are experimentally obtained using system identification method. Their values are presented as follows.

$$\begin{aligned} a_1 &= 21.97, \quad b_1 = 0.2757, \quad c_1 = 22.25 \\ a_2 &= 30.4, \quad b_2 = 0.02994, \quad c_2 = 28.44 \end{aligned}$$

System configuration is shown in Fig. 3. The payload is mounted at the center of tilt gimbal. Its absolute angular position and rate are measured by an Attitude Heading Reference System (AHRS) attached directly.

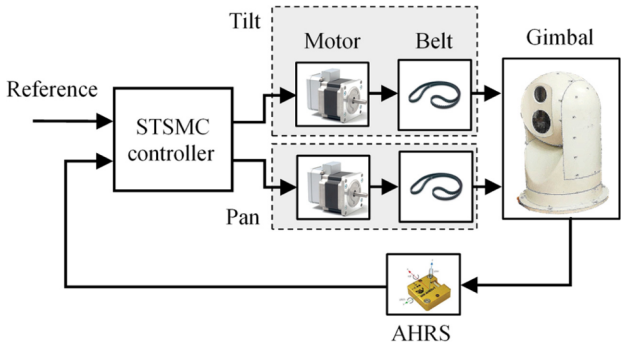

Fig. 3 The configuration of experiment system

Table 1 Experiment system specifications

	Parameter	Value
Actuators: CoolMuscle CM1-C-23S30	Integrated controller	P-PI
	Rated power [W]	45
	Max. speed [rpm]	3000
	Rated continuous torque [Nm]	0.294
	Supply voltage	VDC24±10%
	Supply current [A]	3.9
	Gear ratio	5 : 1
Sensor: NTRexLAB M W-AHRSv1	Measurement algorithm: Fusion of acceleration and gyro sensor with Kalman filter	
	Angle's resolution [°]	0.001
	Static error [°]	0.1
	Dynamic error [°]	2
	Response time [ms]	1

Table 2 Parameters of the proposed controller

Gimbal channel	Tilt	Pan
STSMC	$m_1 = 2$ $\lambda_{11} = 120$ $\lambda_{21} = 100$ $\delta = 5$	$m_1 = 1.5$ $\lambda_{11} = 200$ $\lambda_{21} = 100$ $\delta = 5$
PID	$P_1 = 2.613$ $I_1 = 0.068$ $D_1 = 0.236$ $N_1 = 10$	$P_2 = 2.785$ $I_2 = 0.073$ $D_2 = 0.170$ $N_2 = 10$

Two channels of the gimbal are actuated independently by two servo system through driving belts. There is already a P controller for speed control in each servo as mentioned in Section 3.

All actuators and sensor communicate through RS 232 interface. The controller is implemented in Matlab/Simulink. Sampling time is chosen as 0.05s. The hardware system specifications are listed in Table 1, and the controller gains are represented in Table 2.

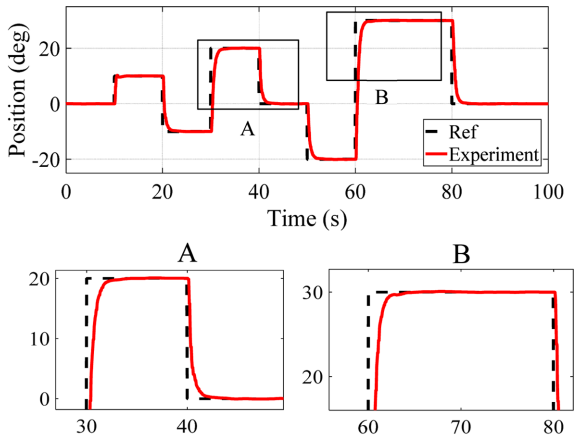

(a) Step response of the tilt

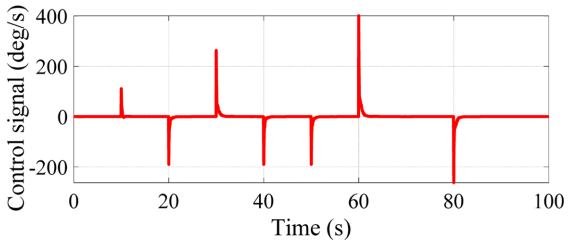

(b) Control signal for the tilt (STSMC controller)

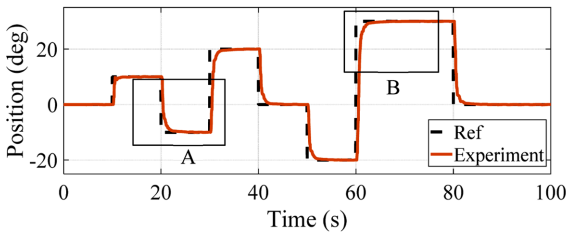

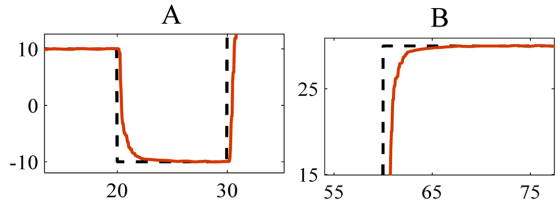

(c) Step response of the pan

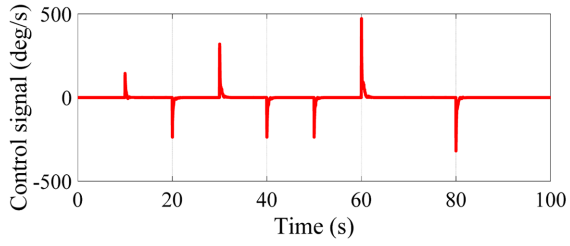

(d) Control signal for the pan (STSMC controller)

Fig. 4 Tracking performance for the step reference signal

At first, two channels are experimented to track target trajectories in forms of step signal value. The response of tilt gimbal and its control signal are shown in Figs. 4(a) and 4(b). Experimental results collected from pan motion are shown in Figs. 4(c) and 4(d). Note that the control signals of the tracking controller are the reference values for the inner stabilizer controllers, so their units are deg/s. One can see that the proposed method achieves desired tracking position in a short time with almost no overshoot. The zoomed figures show in detail the transient responses and steady states of each channel. Evidently, the system is robust and well performed.

Then, a comparison of system performance controlled by STSMC and PID controller is presented to evaluate the efficiency of the proposed control law more clearly. The PID controller has the general form as follows Eq. (27).

$$G_i(s) = P_i + I_i\frac{1}{s} + D_i\frac{N_i}{1+N_i\frac{1}{s}} \tag{27}$$

where tuned controller gains are also represented in Table 2.

Both channels of the gimbal are controlled at the same time so that the LOS tracked a target object following a counterclockwise-circular trajectory in a vertical plane. Tracking performances are shown in Fig. 5. Furthermore, the root-mean-square errors (RMS) of the experiment data are calculated and shown in Table 3.

In Fig. 5(a), the circular trajectory in the vertical plane and corresponding system outputs are presented. At the first glance on the results, the PID control seems to achieve better tracking performance. However, it is worth to notice that the results are shown geometrically only in Fig. 5(a), which may lead to the difficulty in evaluating the system responses with respect to time. The zoomed figures, where the reference point and corresponding system outputs at a specific time are highlighted, show that the tracking error by STSMC is smaller than the error generated by PID controller. It is easy to see that the system response controlled by STSMC is very closed to the reference, while the one by the PID controller is always far behind. The tracking errors in Fig. 5(b) also prove that the STSMC archives significantly better performance.

In detail, Fig. 5(c) shows the angle response of each channel controlled by PID controller is always behind and the one of STSMC is almost match to the reference. In addition, Fig. 5(d) shows the control signals from STSMC and PID controller. The element u_{iST} in the STSMC's control signal compensates unmodelled dynamics and disturbances perturbed the system, which causes the bounce as seen in this Fig. 5.

For the RMS tracking errors shown in Table 3, the proposed STSMC provides much smaller tracking error in both channels. However, the radial residual of PID controller is accidently smaller, due to periodic characteristic of circular trajectory.

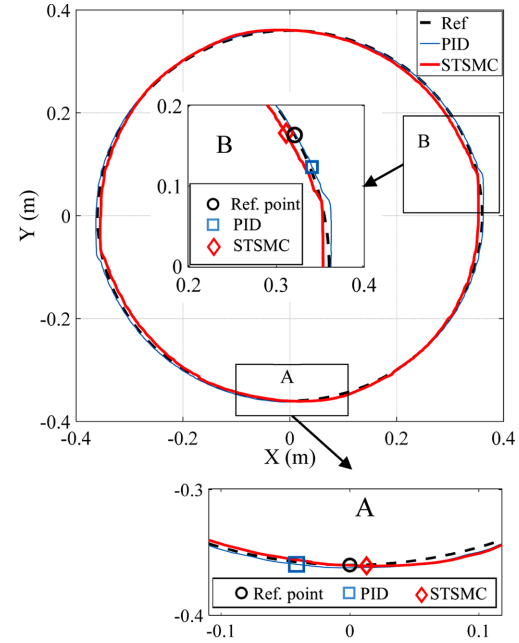

(a) Route tracking performance

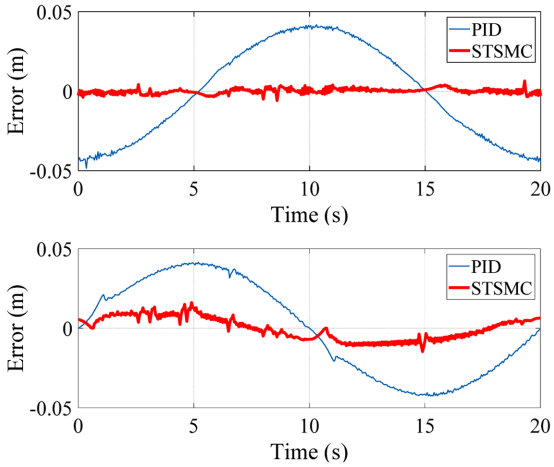

(b) Tracking error of the tilt (above) and the pan (Bellow)

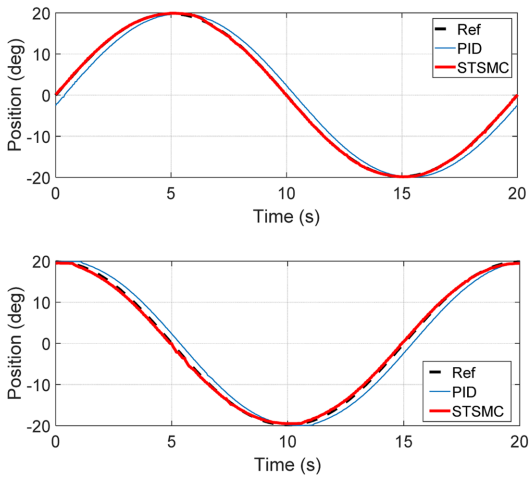

(c) Angle of the tilt (Top) and the pan (Bottom)

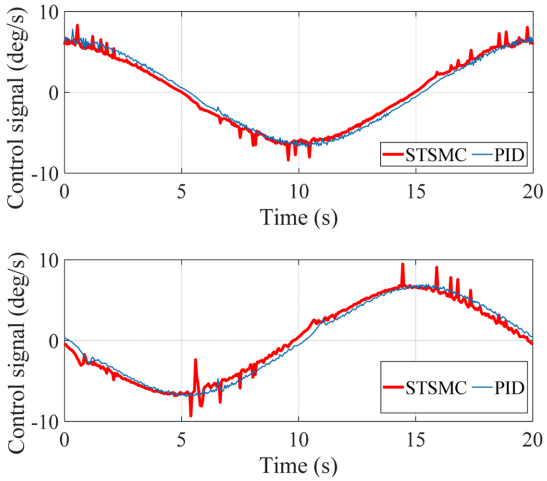

(d) Control signal for the tilt (Top) and the pan (Bottom)

Fig. 5 Tracking performance for a circular reference trajectory

Table 3 RMS values

RMS	Tilt	Pan	Radial
STSMC	0.0017	0.0071	0.0043
PID	0.0298	0.0295	0.0025

7. Conclusions

In this paper, a super-twisting sliding mode controller has been designed for the gimbal motion control. A system model has been obtained from the analysis of system kinematics and dynamics, and consideration of the presence of stabilization controller. By experimental studies, the effectiveness of the proposed controller has been shown and validated. Comparing with tradition PID controller, the designed super-twisting controller has achieved much better performance. In detail, for the tilt and pan channels, the RMS error of the proposed control method is respectively equal to 5.7 and 24% of those from PID control. The system performance robustness with respect to limited disturbances is proved by Lyapunov theory. Consider complex kinematics coupling and outer disturbance influencing the system, future studies are necessary to enhance system performance and robustness.

REFERENCES

1. Hilkert, J., “Inertially Stabilized Platform Technology Concepts and Principles,” IEEE Control Systems Magazine, Vol. 28, No. 1, pp. 26-46, 2008.
2. Kürkçü, B., Kasnakoğlu, C., and Efe, M. Ö., “Disturbance/ Uncertainty Estimator Based Integral Sliding-Mode Control,” IEEE Transactions on Automatic Control, Vol. 63, No. 11, pp. 3940-3947, 2018.
3. Li, H. and Yu, J., “Anti-Disturbance Control based on Cascade ESO and Sliding Mode Control for Gimbal System of Double Gimbal CMG,” IEEE Access, Vol. 8, pp. 5644-5654, 2019.
4. Mao, J., Yang, J., Liu, X., Li, S., and Li, Q., “Modeling and Robust Continuous TSM Control for an Inertially Stabilized Platform with Couplings,” IEEE Transactions on Control Systems Technology, Vol. 28, No. 6, pp. 2548-2555, 2019.
5. Suoliang, G., Lei, Z., Zhaowu, P., and Shuang, Y., “Finite-Time Robust Control for Inertially Stabilized Platform based on Terminal Sliding Mode,” Proc. of the 37th Chinese Control Conference, pp. 483-488, 2018.
6. Dong, F., Lei, X., and Chou, W., “A Dynamic Model and Control Method for a Two-Axis Inertially Stabilized Platform,” IEEE Transactions on Industrial Electronics, Vol. 64, No. 1, pp. 432-439, 2016.
7. Ding, Z., Zhao, F., Lang, Y., Jiang, Z., and Zhu, J., “Anti-Disturbance Neural-Sliding Mode Control for Inertially Stabilized Platform with Actuator Saturation,” IEEE Access, Vol. 7, pp. 92220-92231, 2019.
8. Chalanga, A., Kamal, S., Fridman, L. M., Bandyopadhyay, B., and Moreno, J. A., “Implementation of Super-Twisting Control: Super-Twisting and Higher Order Sliding-Mode Observer-Based Approaches,” IEEE Transactions on Industrial Electronics, Vol. 63, No. 6, pp. 3677-3685, 2016.
9. Tran, M. T., Kim, K. H., Park, H. C., and Kim, Y. B., “A Study on an Adaptive Super-Twisting Sliding Mode Control Design with Perturbation Estimation,” Journal of Power System Engineering, Vol. 24, No. 2, pp. 53-63, 2020.
10. Reis, M. F., Monteiro, J. C., Costa, R. R., and Leite, A. C., “Super-Twisting Control with Quaternion Feedback for a 3-DoF Inertial Stabilization Platform,” Proc. of the IEEE Conference on Decision and Control, pp. 2193-2198, 2018.
11. Levant, A., “Robust Exact Differentiation via Sliding Mode Technique,” Automatica, Vol. 34, No. 3, pp. 379-384, 1998.
12. Moreno, J. A. and Osorio, M., “Strict Lyapunov Functions for the Super-Twisting Algorithm,” IEEE Transactions on Automatic Control, Vol. 57, No. 4, pp. 1035-1040, 2012.
13. Moreno, J. A. and Osorio, M., “A Lyapunov Approach to Second-Order Sliding Mode Controllers and Observers,” Proc. of the 47th IEEE Conference on Decision and Control, pp. 2856-2861, 2008.
14. Seeber, R. and Horn, M., “Stability Proof for a Well-Established Super-Twisting Parameter Setting,” Automatica, Vol. 84, pp. 241-243, 2017.
15. Kennedy, P. J. and Kennedy, R. L., “Direct Versus Indirect Line of Sight (LOS) Stabilization,” IEEE Transactions on Control Systems Technology, Vol. 11, No. 1, pp. 3-15, 2003.
16. Ekstrand, B., “Equations of Motion for a Two-Axes Gimbal System,” IEEE Transactions on Aerospace and Electronic Systems, Vol. 37, No. 3, pp. 1083-1091, 2001.
17. Mokbel, H. F., Ying, L. Q., Roshdy, A. A., and Hua, C. G., “Modeling and Optimization of Electro-Optical Dual Axis Inertially Stabilized Platform,” Proc. of the International Conference on Optoelectronics and Microelectronics, pp. 372-377, 2012.
18. Masten, M. K., “Inertially Stabilized Platforms for Optical Imaging Systems,” IEEE Control Systems Magazine, Vol. 28, No. 1, pp. 47-64, 2008.
19. Fridman, L., Moreno, J., and Iriarte, R., “Sliding Modes after the First Decade of the 21st Century,” Lecture Notes in Control and Information Sciences, Vol. 412, pp. 113-149, 2011.

Thinh Huynh
Graduate School Student in the Department of Smart Robot Convergence and Application Engineering, the Graduate School, Pukyong National University. His research interests include control engineering, robotics and automotive engineering.
E-mail: huynhthinh@hcmute.edu.vn

Young-Bok Kim
Professor in the Department of Mechanical System Engineering, Pukyong National University. His research interests include control theory and application with dynamic ship positioning and autonomous control system design, etc.
E-mail: kpjiwoo@pknu.ac.kr